

## Electronic Supplementary Information (ESI)

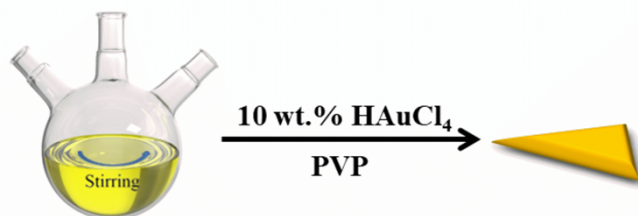
### Experimental Section:

**Materials and instrumentation.** Chloroauric acid ( $\text{HAuCl}_4 \cdot 4\text{H}_2\text{O}$ ), chloroplatinic acid ( $\text{H}_2\text{PtCl}_6 \cdot 6\text{H}_2\text{O}$ ), trisodium citrate (cit), L-Ascorbic acid (AA), 1,5-pentadiol ( $\text{C}_5\text{H}_{12}\text{O}_2$ ) and ethanol ( $\text{C}_2\text{H}_5\text{OH}$ ) were purchased from Sinopharm Chemical Reagent Co, Ltd (China). Mercaptosuccinic acid (MSA), polyvinylpyrrolidone (PVP, molecular weight 36000) were obtained from Sigma-Aldrich Co. All chemicals were of analytical grade and used without further purification. All aqueous solutions were prepared using Milli-Qwater.

Scanning electron microscopy (SEM image was captured under Hitachi S-4700 with accelerating voltage of 5 kV). Transmission Electron Microscopy (The TEM model HT7700, manufactured by Hitachi Corporation of Japan). The electrochemical experiments were conducted using the CHI631B electrochemical workstation. Raman spectra were recorded using confocal micro-Raman system (XploRA PLUS, Jobin Yvon, France). The microscope attachment, which was based on an Olympus BX40 system, used  $\times 50$  long-working-length objective ( $\sim 8$  mm). All experiments were carried out at excitation line of 638 nm from internal He-Ne laser with power of 3.77 mW.

### Synthesis of Au plate

The Au plate were synthesized via hydrothermal reduction of polyols<sup>[1,2]</sup>: Transfer 9 mL of 1,5-pentadiol into 25 mL single-neck flask and add 0.60 g of PVP. Stir the mixture continuously while heating it to  $155^\circ\text{C}$ , then rapidly introduce 1 mL of 10 wt.%  $\text{HAuCl}_4$  aqueous solution. After approximately 25 minutes, substantial quantity of Au plates become discernible within the solution. Proceed for 1 h and subsequently expedite the transfer to ice bath for rapid cooling. The preparation process is illustrated in Scheme S1.



Scheme S1. Schematic diagram of synthesis of Au plate.

As can be seen from Fig. S1, the Au plate exhibits triangular cross-section with

dimensions of approximately 10  $\mu\text{m}$  and thickness of around 250 nm. Furthermore, its surface possesses atomic smoothness devoid of any defects, rendering it suitable as the plane base for nanoparticle collisions.

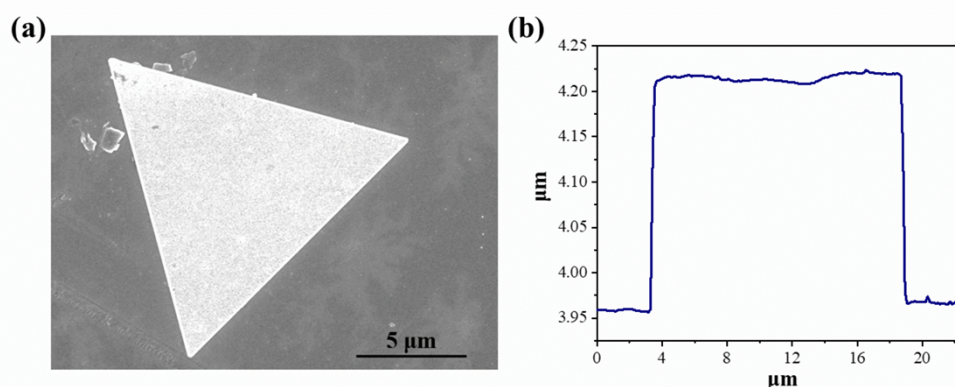


Fig. S1 (a) SEM image of Au plate. (b) Sectional height map of Au plate characterized by AFM.

### Synthesis of Au@Pt nanoparticles

The classical Frens method was employed for the synthesis of 15 nm Au nanoparticle seeds<sup>[3]</sup>: 0.01 wt.%  $\text{HAuCl}_4$  aqueous solution was placed in 250 mL three-neck flask, heated to boiling and maintained for 15 minutes. Then, rapidly added was 2 mL of 1 wt.% cit aqueous solution, resulting in the colorless solution turning black and finally Burgundy. The stirring continued for another half an hour to obtain Au seeds liquid with size of 15 nm, which was then cooled naturally and stored in the refrigerator.

Au nanoparticles (Au NPs) were synthesized via the seed growth method<sup>[4]</sup>: 2 mL of 15 nm Au seeds, prepared using the Frens method, were placed in 100 mL three-neck flask. Subsequently, 10 mL of 0.1 wt.%  $\text{HAuCl}_4$  aqueous solution was added and the mixture was vigorously stirred at room temperature for 5 minutes to ensure homogeneity. Following this, an additional 36 mL of ultra-pure water was added and stirring continued for another 5 minutes. Finally, by introducing 1.5 mL of  $0.01 \text{ mol} \cdot \text{dm}^{-3}$  MSA solution and stirring for duration of 40 minutes, Au nanoparticles with average size of approximately 55 nm were successfully synthesized. The preparation process is illustrated in Scheme S2.

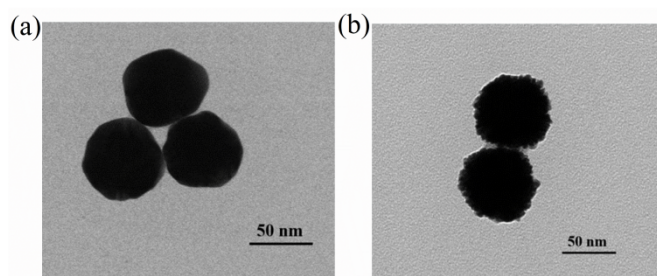
Au@Pt nanoparticles (Au@Pt NPs) were synthesized via hydrothermal synthesis method<sup>[5]</sup>: Take 30 mL of Au nanoparticles with size of 55 nm and introduce 6 mL of  $1 \text{ mmol} \cdot \text{dm}^{-3}$   $\text{H}_2\text{PtCl}_6 \cdot 6\text{H}_2\text{O}$  aqueous solution into 100 mL three-neck flask. Vigorously stir the mixture at  $80^\circ\text{C}$  for 8 minutes to achieve homogeneity. Injection pump was employed to gradually add 3.5 mL of  $10 \text{ mmol} \cdot \text{dm}^{-3}$  AA aqueous solution at rate of  $30 \text{ mL} \cdot \text{h}^{-1}$  dropwise. After completing the drip addition, continue stirring the aqueous solution at this temperature for additional duration of 40 minutes before cooling it down to room temperature in order to obtain Au@Pt NPs. The thickness of its shell measures

approximately 4 nm.



Scheme S2. Schematic diagram of synthesis of Au nanoparticles.

As can be seen from Fig. S2(a), the Au NPs reduced by MSA exhibit quasi-spherical morphology with relatively smooth surface. However, upon the growth of Pt NPs on the Au NPs surface, the resulting structure becomes rough and exhibits loose arrangement (Fig. S2(b)). The core-shell structure of Au@Pt NPs were characterized using energy-dispersive X-ray spectroscopy (EDS) elemental surface mapping tests. As depicted in Fig. S2(c), (e) and (f), the distribution of Au is predominantly centered within the core region (red), while Pt is primarily localized on the shell region (green). The EDS line-scan region indicated by the green arrow in Fig. S2(c) confirms that higher content of Au is detected in the central region, while higher content of Pt is appeared at the edge (Fig. S2(d)). This outcome unequivocally verifies the presence of core-shell architecture in the Au@Pt NPs, comprising an inner core composed of Au and an outer shell comprised of Pt. The shell thickness measures approximately 4 nm, and the CV diagram of Au@Pt nanoparticles reveals no REDOX peak for Au, only a reduction peak for Pt oxide. It indicates that the Pt shell tightly coats the surface of the prepared Au@Pt nanoparticles without any pinholes (Fig. S3(a)). The Pt wire serves as the counter electrode, and the saturated calomel electrode (SCE) is used as the reference electrode. The scanning rate of  $50 \text{ mV}\cdot\text{s}^{-1}$  is applied. Compared to Au NPs, the SERS effect of Au@Pt NPs were found to be reduced, however, Au@Pt NPs still exhibited commendable SERS activity and thus hold potential as valuable research materials for SERS (Fig. S3(c)).



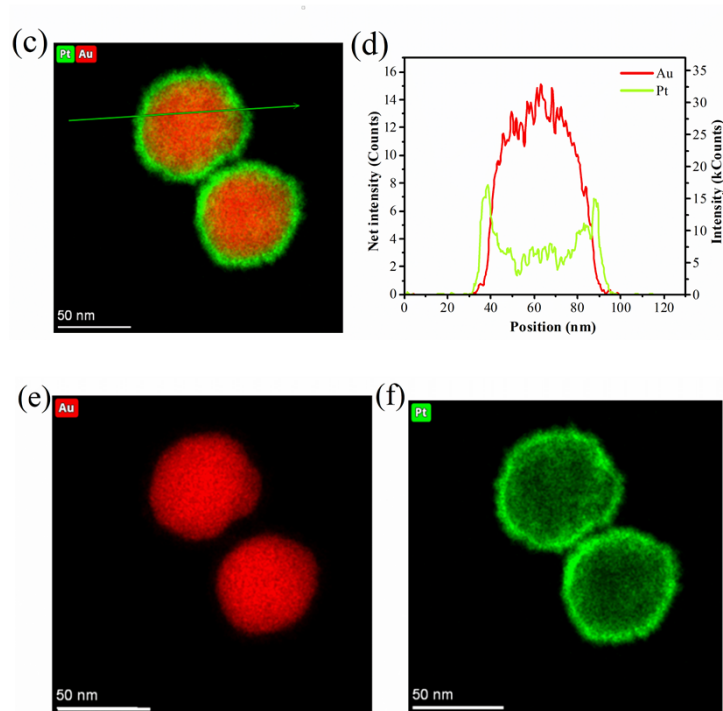


Fig. S2 TEM images (a) Au NPs; (b) Au@Pt NPs. (c), (e) and (f) EDS element distribution map of Au@Pt NPs. (d) Distribution of EDS element content in the green arrow line-scan in Fig.S2(c).

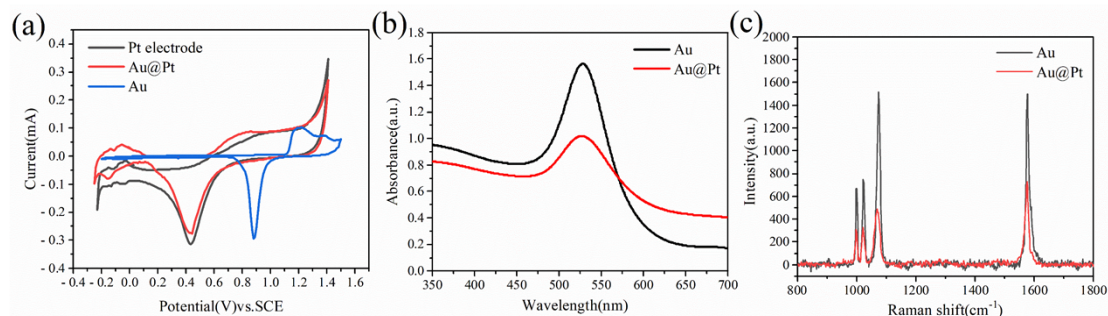


Fig. S3 (a) Cyclic voltammogram curves of Au NPs, Au@Pt NPs and Pt electrode in  $0.5 \text{ mol} \cdot \text{dm}^{-3}$   $\text{H}_2\text{SO}_4$  solution (Scanning rate:  $50 \text{ mV} \cdot \text{s}^{-1}$ ). (b) Ultraviolet-visible spectra of Au NPs and Au@Pt NPs. (c) SERS spectra of TP molecules on the surface of Au NPs and Au@Pt NPs (Concentration of TP:  $1 \text{ mmol} \cdot \text{dm}^{-3}$ ).

## The surface of the Au UME before and after modified Au plate

The Au UME surface is positioned beneath the  $\times 50$  microscope lens of the Raman spectrometer, as depicted in Fig. S4(a).  $10 \mu\text{L}$  droplets of the previously prepared Au plate solution are carefully added onto the ultramicroelectrode surface. Through microscopic observation, successful assembly of the Au plate onto the Au UME surface can be observed with one or multiple time, thereby obtaining Au plate modified Au UME as shown in Fig. S4(b).

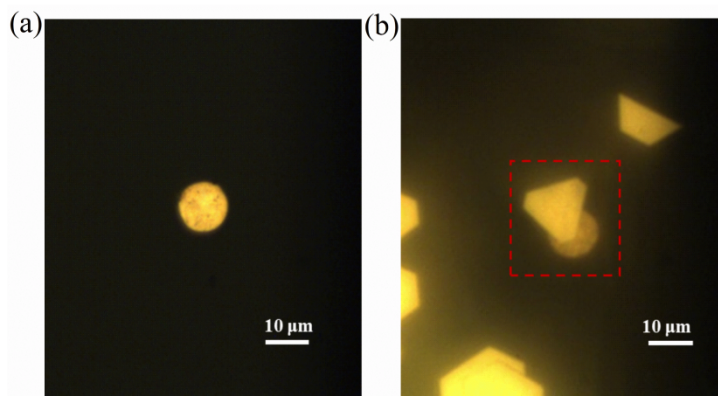


Fig. S4 Photograph images of Au UME before (a) and after (b) modified Au plate under the  $\times 50$  telephoto microscope lens of Raman spectrometer.

## Experiment schematic diagram

The Au@Pt nanoparticle-Au plate collision system installation, as depicted in Fig. S5, is conducted within self-assembled cylindrical vessel measuring 3 cm in diameter and 1 cm in height. A glass elbow fixed on the side facilitates liquid addition and placement of the reference saturated calomel electrode. The working electrode is 12.5  $\mu\text{m}$  Au UME in diameter. The electrolyte employed is  $\text{N}_2$  saturated  $1 \text{ mmol} \cdot \text{dm}^{-3} \text{H}_2\text{SO}_4$  solution. The Raman spectrometer laser is precisely focused on the surface of the Au plate through glass window located at the upper end of the cylindrical container, thereby enabling simultaneous monitoring of SERS and current.

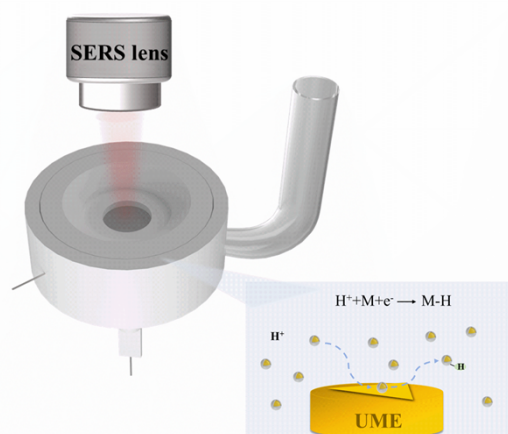


Fig. S5 Schematic diagram of SERS measurement of Au@Pt nanoparticle-Au plate collisions.

## Verification of the Pt-H bond

Au@Pt NPs were assembled on the surface of glassy carbon electrode (Au@Pt NPs/GC electrode) with diameter 3 mm and subjected to test in  $\text{D}_2\text{O}$  solution containing  $1 \text{ mmol} \cdot \text{dm}^{-3} \text{D}_2\text{SO}_4$ . SERS spectra were obtained under different potentials, as depicted in Fig. S8. The SERS peaks observed at  $1175 \text{ cm}^{-1}$  and  $2490 \text{ cm}^{-1}$  can be

attributed to the bending vibration of D<sub>2</sub>O, while the SERS peak at 1415 cm<sup>-1</sup> is indicative of the stretching vibration of Pt-D bond [6]. Notably, no SERS peak was observed at 2075 cm<sup>-1</sup>. This observation confirms that the previously measured spectral peak at 2075 cm<sup>-1</sup> in 1 mmol·dm<sup>-3</sup> H<sub>2</sub>SO<sub>4</sub> solution is indeed associated with the vibrational mode of Pt-H bond.

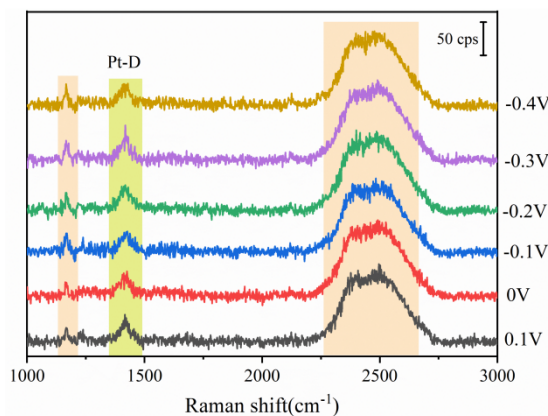


Fig. S6 The potential-dependent SERS spectra on Au@Pt NPs/GC electrode (Solution: 1 mmol·dm<sup>-3</sup> D<sub>2</sub>SO<sub>4</sub>+D<sub>2</sub>O).

### The potential-dependent SERS spectra of Pt-H bond

The SERS peak frequency exhibited redshift from 2081 cm<sup>-1</sup> to 2053 cm<sup>-1</sup> during the dynamic monitoring of Pt-H bond, as the potential was shifted from 100 mV to -500 mV. According to the literature [7, 8], this sensitivity arises from the spectral characteristics of Pt-H being highly dependent on surface coverage. Surface hydrogen not only interacts with Pt atoms and adjacent hydrogen, but also with electrolyte ions and water molecules. Thus, the observed red-shift of Pt-H band with negative movement of potential should be attributed to the lateral interaction of Pt-H bonds of different coverage.

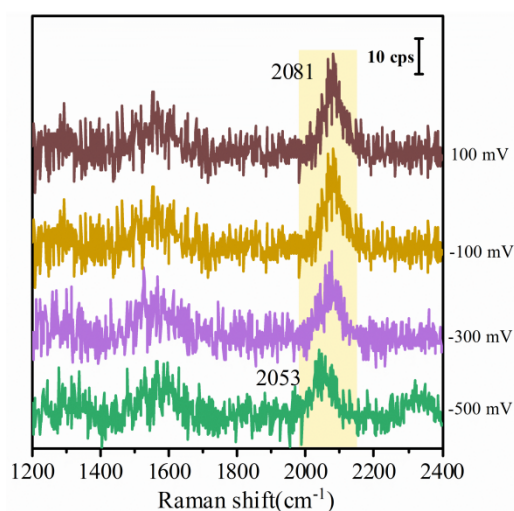


Fig. S7 The potential-dependent SERS spectra of Pt-H bond.

## Estimation on contribution of single collision and SERS intensity of single Pt-H

Using the finite element method, we simulate the coupling between single Au@Pt NP and Au plate. When the diameter of the Au@Pt NP is 63 nm and its distance from the Au plate is 0.9 nm (equivalent to the length of AA molecule on the surface of the Au@Pt NP), we observe enhancement factor (EF) in the “hot spot” region electromagnetic field ranging from  $1.8 \times 10^4$  to  $1.8 \times 10^6$ . The scattering cross-section radius of this “hot spot” is approximately 13 nm (Fig. S8(a-b)), with area given by  $S_{\text{hot spot}} = \pi \times (13 \text{ nm})^2 = 530.66 \text{ nm}^2$ .

① Total electrode area:

The Au plate in Fig. S4(b) depicts coating with diameter of 10  $\mu\text{m}$  on the surface of Au UME measuring 12.50  $\mu\text{m}$  in diameter. Considering the uncovered portion of the microelectrode, the Au plate can be regarded as trapezoid with dimensions: height = 5  $\mu\text{m}$ , and sides = 5  $\mu\text{m}$  and 10  $\mu\text{m}$  respectively. Consequently, upon assembly of the Au plate, the estimated total electrode area is given by  $S_{\text{total}} = S_{\text{UME}} + S_{\text{Au plate}} = \pi \times (12.50 \mu\text{m} / 2)^2 + ((5 \mu\text{m} + 10 \mu\text{m}) \times 5 \mu\text{m}) / 2 \approx 160 \mu\text{m}^2 = 1.60 \times 10^8 \text{ nm}^2$ .

② Raman laser spot area:

The SERS test lens utilized in the experiment is  $\times 50$  long-focus objective lens. The diameter of the circular laser spot can be calculated using the formula  $d = (1.22 \lambda) / N_A$ , where  $\lambda$  represents the laser wavelength (638 nm) and  $N_A$  denotes the numerical aperture of the objective lens (0.6). Substituting these values yields  $d = 1.30 \times 10^3 \text{ nm}$ . Consequently, the area of the circular laser spot can be approximated as  $S_{\text{laser}} = \pi \times (d / 2)^2 \approx 1.32 \times 10^6 \text{ nm}^2$ .

③ Surface area of Au@Pt NPs:

The surface area of spherical Au@Pt nanoparticles with diameter of 63 nm can be calculated as  $S_{\text{Au@Pt}} = 4\pi r^2 = 4 \times 3.14 \times (63 \text{ nm} / 2)^2 \approx 1.20 \times 10^4 \text{ nm}^2$ .

④ The amount of charge transferred by single Au@Pt surface:

The electric charge density of hydrogen atoms adsorbed on Pt in complete monolayer configuration is measured to be 210  $\mu\text{C} \cdot \text{cm}^{-2}$ , equivalent to  $2.10 \times 10^{-18} \text{ C} \cdot \text{nm}^{-2}$ . Upon collision between single Au@Pt nanoparticle and the electrode surface, the amount of charge that can be transferred is estimated to be approximately  $2.10 \times 10^{-18} \text{ C} \cdot \text{nm}^{-2} \times 1.20 \times 10^4 \text{ nm}^2 \approx 2.52 \times 10^{-14} \text{ C}$ .

⑤ SERS intensity contribution of single collision between Au@Pt and Au plate:

The integrated current “spike” signal observed at the 380th second after the addition of Au@Pt NPs to Fig. 1 (Fig. S8(d)) exhibits area of  $2.01 \times 10^{-11}$ , indicating theoretical charge transfer by Au@Pt NPs upon collision with the entire electrode

surface is  $2.01 \times 10^{-11}$  C. Since SERS exclusively captures the Pt-H generated by the collision between Au@Pt NPs and the electrode surface within the laser spot, in theory, the charge transferred during this collision between Au@Pt nanoparticles and the electrode surface in the laser spot region is calculated as  $2.01 \times 10^{-11} \text{ C} \times (1.32 \times 10^6 \text{ nm}^2) / (1.60 \times 10^8 \text{ nm}^2) = 1.66 \times 10^{-13} \text{ C}$ . The electric charge of  $1.66 \times 10^{-13} \text{ C}$  is generated by the  $1.66 \times 10^{-13} \text{ C} / 2.52 \times 10^{-14} \text{ C} \approx 7$  times effective collision between Au@Pt and the electrode in the laser spot range. According to the SERS signal intensity of Pt-H vibration measured at the 380th (Fig. S8(c)), the theoretical contribution of single collision between Au@Pt and Au plate to SERS intensity can be calculated as  $26.34 \text{ cps} / 7 \approx 3.73 \text{ cps}$ .

⑥ SERS intensity contribution of single Pt-H bond:

The electric charge density of hydrogen atoms adsorbed on Pt in complete monolayer configuration is measured to be  $210 \mu\text{C} \cdot \text{cm}^{-2}$ , equivalent to  $2.10 \times 10^{-18} \text{ C} \cdot \text{nm}^{-2}$ . The Volmer reaction, represented by  $\text{H}_3\text{O}^+ + \text{e}^- + \text{M} \rightarrow \text{M-H} + \text{H}_2\text{O}$ , involves single electron transfer process, where the charge of an elementary charge  $e$  is  $1.60 \times 10^{-19} \text{ C}$ . Consequently, the number of hydrogen atoms adsorbed on Pt surface with area of  $1 \text{ nm}^2$  in full monolayer arrangement is calculated as  $(2.10 \times 10^{-18} \text{ C} \cdot \text{nm}^{-2}) / (1.60 \times 10^{-19} \text{ C}) \approx 13$ . Assuming monolayer of fully adsorbed H atoms on the Pt surface,  $S_{\text{“hot spot”}}$  =  $530.66 \text{ nm}^2$ , then the number of Pt-H in the “hot spot” of single Au@Pt nanoparticle colliding with Au plate is  $530.66 \times 13 = 6989$ , and each Pt-H contributes to SERS intensity of about  $3.73 \text{ cps} / 6989 \approx 5.34 \times 10^{-4} \text{ cps}$ .

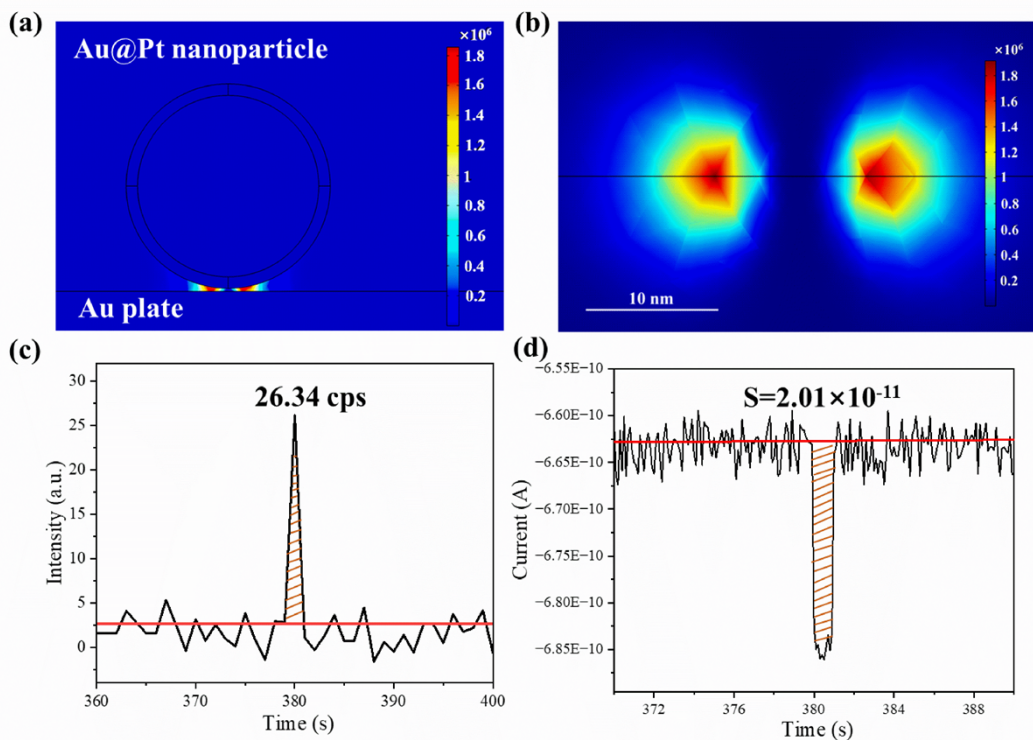


Fig. S8 (a, b) Electromagnetic field intensity distribution map in nanogap between Au@Pt nanoparticle and Au plate. (c) The time-dependent SERS trajectory of 360 s-400 s. (d) The time-dependent current trajectory of 370 s-390 s. (The data obtained from the addition of Au@Pt nanoparticles in Fig. 1)

## References

1. C. C. Li, W. P. Cai, B. Q. Cao, F. Q. Sun, Y. Li, C. X. Kan and L. D. Zhang, *Adv. Funct. Mater.*, 2005, **16**, 83-90.
2. A. R. Tao, S. Habas and P. Yang, *Small*, 2008, **4**, 310-325.
3. G. Frens, *Nat. Phys. Sci.*, 1973, **241**, 20-22.
4. J. L. Niu, T. Zhu and Z. F. Liu, *Nanotechnology*, 2007, **18**, 325607-325614.
5. J. F. Li, Z. L. Yang, B. Ren, G. K. Liu, P. P. Fang, Y. X. Jiang, D. Y. Wu and Z. Q. Tian, *Langmuir*, 2006, **22**, 10372-10379.
6. J. F. Li, Y. F. Huang, S. Duan, R. Pang, D. Y. Wu, B. Ren, X. Xu and Z. Q. Tian, *Phys. Chem. Chem. Phys.*, 2010, **12**, 2493-2502.
7. B. Ren, X. Xu, X. Q. Li, W. B. Cai and Z. Q. Tian, *Surf. Sci.*, 1999, **427-28**, 157-161.
8. X. Xu, B. Ren, D. Y. Wu, H. Xian, X. Lu, P. Shi and Z. Q. Tian, *Surf. Interface Anal.*, 1999, **28**, 111-114.